Geological Society of America
Memoir 194
2001

Kinematics of exhumation of high- and ultrahigh-pressure rocks in the Hong'an and Tongbai Shan of the Qinling-Dabie collisional orogen, eastern China

Laura E. Webb*
Department of Geological and Environmental Sciences, Stanford University, Stanford, California, 94305-2115, USA
Lothar Ratschbacher
Institut für Geologie, Technische Universität, Bergakademie Freiberg, Bernhard von Cottastrasse 2, D-09596, Freiberg, Germany
Bradley R. Hacker
Department of Geological Sciences, University of California at Santa Barbara, Santa Barbara, California, 93106-9630, USA
Shuwen Dong
Institute of Geomechanics, Chinese Academy of Geological Sciences No. II, Ming zhu Xueyang South Road, 100081 Beijing, China

ABSTRACT

The Hong'an region offers an unique opportunity to investigate the tectonics of the continental collision event preserved in high-pressure (*P*) and ultrahigh-*P* metamorphic rocks in the Qinling-Dabie orogen of eastern China. Here, the extensive Cretaceous tectonic and thermal overprint observed in the Dabie Shan is weak. Normal-sense shear along the north-dipping Huwan detachment zone at the northern edge of the Hong'an block occurred ca. 235 Ma. This detachment facilitated the bulk of the exhumation of the high- and ultrahigh-*P* rocks as a penetratively deformed slab. The high- and ultrahigh-*P* rocks are exposed in a warped extensional footwall within which kinematic indicators in the high- and ultrahigh-*P* units show approximately top-to-north shear. Deformation was accompanied by retrograde metamorphism at amphibolite to greenschist facies conditions. Locally, younger northeast-southwest subhorizontal extension is recorded in ductile to brittle fabrics and the timing of deformation is defined by white mica recrystallization ca. 195 Ma. An Early Cretaceous dextral shear zone along the southwest boundary of the Tongbai Shan was synchronous with plutonism and normal to sinistral-oblique slip along the Xiaotian-Mozitang fault, which forms the northern boundary of the Dabie Shan. Coeval dextral and sinistral shear zones along the southwestern and northern margins of these blocks would have caused eastward lateral extrusion of the Tongbai, Hong'an, and Dabie Shan, perhaps driven by collision of the Lhasa block with Eurasia.

INTRODUCTION

Metamorphic diamond and coesite in ultrahigh-pressure (*P*) rocks of the Qinling-Dabie orogen attest to exhumation of subducted continental crust from depths >100 km (e.g., Xu et al., 1992; Wang and Liou, 1991). Preservation of ultrahigh-*P* metamorphic assemblages requires cooling during decompression. This may be achieved by specific tectonic scenerios such as continued underthrusting beneath the ultrahigh-*P* rocks to suppress heating and/or exhumation of ultrahigh-*P* rocks in the lower plate of an extensional shear zone (Platt, 1986; Hacker

*Current address: Department of Earth Sciences, Heroy Geology Laboratory, Syracuse University, Syracuse, New York, 13244-1070, USA

Webb, L.E., et al., 2001, Kinematics of exhumation of high- and ultrahigh-pressure rocks in the Hong'an and Tongbai Shan of the Qinling-Dabie collisional orogen, eastern China, *in* Hendrix, M.S., and Davis, G.A., eds., Paleozoic and Mesozoic tectonic evolution of central Asia: From continental assembly to intracontinental deformation: Boulder, Colorado, Geological Society of America Memoir 194, p. 231–245.

and Peacock, 1994). Because of the wide variety and large volume of continental rocks metamorphosed at ultrahigh-*P* conditions, the Hong'an region of the orogen provides an excellent opportunity to address the kinematics of deformation within the deepest levels of the collision. In addition to the study of ultrahigh-*P* tectonics, determining the kinematics and timing of events in this complex region is important for understanding the Mesozoic tectonic evolution of Asia. In this chapter we present new structural data from the Hong'an and Tongbai Shan that are critical to determining which tectonic mechanisms were responsible for the exhumation of the ultrahigh-*P* rocks. The timing of deformation is determined by geochronological data discussed in detail in Webb et al. (1999), Hacker et al. (2000), and Ratschbacher et al. (2000). These data define the geometry, kinematics, and timing of tectonism.

REGIONAL GEOLOGY

The 2000 km northwest-trending Qinling orogen marks the boundary between the Precambrian Sino-Korean and Yangtze cratons (Fig. 1). This composite orogen is characterized by the juxtaposition of the ca. 400 Ma north Qinling–Tongbai metamorphic belt and the ca. 220 Ma south Qinling–Dabie metamorphic belt (Mattauer et al., 1985; Zhai et al., 1998). The south Qinling–Dabie complex formed during Triassic collision between the Yangtze and Sino-Korean cratons. Paleomagnetic data suggest that the Yangtze and Sino-Korean cratons did not fully converge until at least Late Triassic time (Lin et al., 1985; Opdyke et al., 1986) and that the Yangtze craton was oriented ~60° counterclockwise from its present orientation prior to the Middle Triassic. These data suggest that the collision progressed from east to west, closing the intervening oceanic basin as the Yangtze craton rotated with respect to the Sino-Korean craton (e.g., Enkin et al., 1992).

During collision, ultrahigh- and high-*p* metamorphic rocks formed in a north-dipping subduction zone. These rocks are exposed in the easternmost Tongbai, Hong'an, Dabie, and Su-Lu ranges, but transitional blueschist-greenschist facies rocks extend for ~600 km along the southern margin of the orogen through the Tongbai and Qinling areas (e.g., Dong, 1989; Ernst et al., 1991; Fig. 1). The high- and ultrahigh-*P* metamorphic rocks form the core of the Qinling-Dabie orogen in the Dabie Shan and Hong'an regions. North-dipping detachment fault zones define the northern topographic limit of both regions and separate high-grade rocks to the south from greenschist facies and amphibolite facies rocks to the north (cf. Hacker et al., 1996) (Fig. 1). Regionally, the high- and ultrahigh-*P* units trend subparallel to the northwest trend of the orogen. Inferred metamorphic pressures and temperatures increase northward and range from blueschist grade to coesite-eclogite facies rocks (Fig. 1; see Eide [1993] and Liou et al. [1996] for details of the petrologic data). Peak pressures are recorded in eclogite bodies that occur as outcrop-scale blocks or boudins within phengite and/or biotite quartzofeldspathic schists, gneisses, and marbles; locally, eclogites and paragneisses also contain the ultrahigh-*P* indicator minerals coesite and diamond (e.g., Wang and Liou, 1991; Xu and Su, 1997). These features suggest that the eclogites and host paragneisses are part of a crustal sequence that was subducted, metamorphosed, and exhumed together. Each unit has undergone retrograde amphibolite and greenschist facies metamorphism, and all are intruded by Cretaceous plutons (Hacker et al., 1995). The Cretaceous plutonism is coeval with northwest-southeast extension, most pronounced in the Dabie Shan, where synkinematic plutons of intermediate compositions form the northern half of the range (Hacker et al., 1998).

The Tan-Lu fault marks the eastern boundary of the Dabie Shan (Fig. 1). Approximately 500 km of sinistral strike-slip motion during the Triassic–Jurassic has been postulated on the basis of the apparent offset of the Dabie and Su-Lu ultrahigh-*P* terranes (Okay et al., 1993; Yin and Nie, 1993) (Fig. 1). The tectonic significance and age of this fault are still a matter of debate. Although no Triassic–Jurassic structures associated with the Tan-Lu fault have been identified in the Dabie Shan, the Cenozoic Tan-Lu is morphologically well expressed by steep, eastward-dipping faults with normal to dextral-oblique displacement (Ratschbacher et al., 2000). Cenozoic west-northwest–striking, sinistral strike-slip faults conjugate to the Tan-Lu fault are related to the India-Asia collision (e.g., Zhang et al., 1995).

Radiometric data on the timing of collision

The timing of ultrahigh-*P* metamorphism resulting from collision between the Yangtze and Sino-Korean cratons is documented by a growing body of radiometric ages in the range of 245–170 Ma (Li et al., 1989, 1993; Chen et al., 1992; Okay et al., 1993; Eide et al., 1994; Hacker and Wang, 1995; Ames et al., 1996; Rowley et al., 1997; Xue et al., 1997; Hacker et al., 1998, 2000; Webb et al., 1999; Ratschbacher et al., 2000). Ames et al. (1996) and Rowley et al. (1997) reported U/Pb zircon ages of ca. 220 Ma from ultrahigh-*P* eclogites and host gneisses in the Dabie Shan and interpreted these to be the age of peak ultrahigh-*P* metamorphism. Hacker et al. (1998) found a second population of ca. 240 Ma metamorphic overgrowths on single zircon grains from the ultrahigh-*P* unit in the Hong'an and Dabie Shan using a sensitive high-resolution ion microprobe (SHRIMP). The Early Triassic zircon ages agree with Sm/Nd ages of ca. 245 Ma reported by Li et al. (1993) and Okay et al. (1993) and are postulated to represent the timing of ultrahigh-*P* metamorphism. Thus, the radiometric data suggest that the continental collision may have initiated by the end of the Permian.

DATA AND INTERPRETATIONS

Methods

Field work included several north-south transects across the structural grain of the Hong'an and Tongbai Shan to evaluate the development of structures with respect to metamorphism

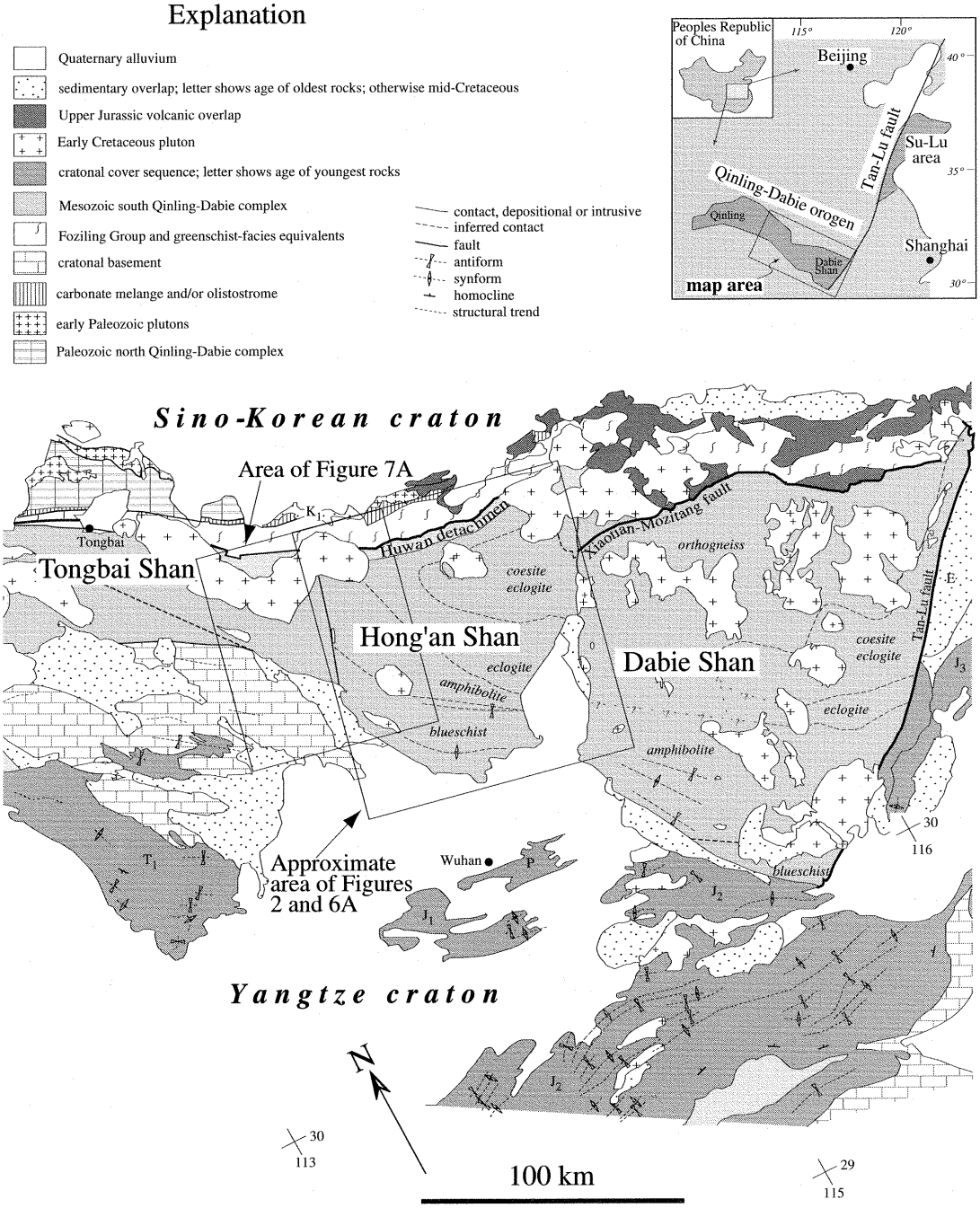

Figure 1. Regional geologic-tectonic map of Qinling-Dabie orogen comprising Tongbai, Hong'an, and Dabie Shan regions. Adapted from Hacker et al. (1995).

and plutonism. These transects included mapping, measurement, and documentation of foliations, lineations, faults and shear zones, and folds, and their relative ages and types. Shear sense was determined from features such as schistosité-cisaillement fabrics, shear bands, and offset dikes and veins. In domains of homogeneous deformation, shear sense was assessed from rotated and/or asymmetric features such as sigma and delta clasts. Mesoscopic fault-slip data were collected to understand fault arrays. The orientation and sense of slip on faults were used to calculate principal stress orientations and shape factors, qualitatively describing the stess geometry. (See Passchier and Trouw [1996] and Angelier [1994] for comprehensive summaries and critical discussions of these structural methods.) Oriented samples of igneous and metamorphic rocks were collected for further analyses, including petrography, microstructural analyses, and $^{40}Ar/^{39}Ar$ geochronology.

Structural observations

Blueschist unit. The blueschist unit consists of blueschist and transitional blueschist-greenschist facies rocks that form the southern third of the Hong'an Shan (Fig. 1; Eide, 1993). The majority of rocks we observed in the blueschist unit were characterized by gneisses and schists of intermediate compositions including high-*P* assemblages of quartz + epidote + phengite + albite ± actinolite ± biotite ± garnet ± Na-amphibole ± titanite ± rutile.

Eide (1993) outlined the structure of the blueschist unit based on studies of exposures at Mulan Shan (Fig. 2A); that structural description is corroborated by our regional study. The blueschist unit is characterized by schist and gneiss that are both lineated and foliated (LS tectonites), in which S1 foliations are penetrative and defined by planar minerals and compositional banding. Mineral lineations (L1) are defined by glaucophane and muscovite. Both foliation and lineation are folded around shallowly southeast- or northwest-plunging B2 folds (Fig. 3A). No folds considered B1 generation were measured or observed in the field. The asymmetry of B2 folds indicates vergence that is generally to the north, with the exception of one locality where south vergence was observed (Figs. 3A and 4A). A second foliation (S2), or crenulation cleavage, is axial planar to B2 folds (Fig. 3A) and formed during progressive deformation of the blueschist unit (Eide, 1993). Locally, a secondary lineation (L2) is defined by quartz and chlorite and plunges gently to the southwest (Fig. 3). Late-stage veins filled with quartz and chlorite postdate B2 folds and indicate subhorizontal northeast-southwest extension.

In thin section, S1 foliations are typically openly folded and deformation is concentrated along layers of fine-grained quartz and mica. Quartz grains display dynamic recrystallization and in some rocks these fabrics are partially annealed (Fig. 4B). Syntectonic retrograde metamorphism resulted in the chlorite growth in the late stage of this progressive deformation.

Eide et al. (1994) reported phengite $^{40}Ar/^{39}Ar$ cooling ages of 225.1 ± 0.4 Ma and 222.0 ± 0.3 Ma (total fusion ages) from blueschists at Mulan Shan. A weighted mean $^{40}Ar/^{39}Ar$ cooling age of 171 ± 2 Ma was obtained from K-feldspar at locality D249 (Table 1; Webb et al., 1999).

Amphibolite unit. In Hong'an, greenschist to epidote-amphibolite facies rocks predominate in a northwest-trending, southwest-dipping zone between the blueschist unit and the eclogite-bearing schists and gneisses to the north (Fig. 1; Eide et al., 1994). Lithologically, this zone is dominated by epidote-chlorite-albite schists and quartzofeldspathic schists and gneisses. Mafic assemblages constitute fine layers and/or occur as blocks. Foliations dip predominately southwest and northeast, reflecting folding around approximately northwest-trending, tight, northeast-vergent B2 folds (Fig. 3B). Stretching lineations include early southeast-plunging lineations that are typically associated with the high-*P* mineral assemblage and subparallel to the B2 folds (Figs. 2 and 3B). They impose apparent dextral transpression on the southwest-dipping foliation. These L1 lineations display progressive overprinting by south- and southwest-plunging lineations associated with the retrogressive mineral assemblage; they impose apparent sinistral transpression (Figs. 2 and 3B). North-directed shear sense within the gneisses and mylonites from this zone and those along the southern margin of the high-*P* eclogite is indicated by shear bands, as well as by mesoscopic and microscopic σ and δ clasts (e.g., Fig. 4C). In felsic lithologies, albite is found as both synkinematic porphyroclasts, at times showing core-mantle structures and recrystallization (Fig. 4C), or as synkinematic to postkinematic porphyroblasts (Fig. 4D). This suggests that deformation occurred at temperatures of 400–500 °C (e.g., Passchier, 1982; Tullis and Yund, 1991), and that locally cooling may have postdated deformation. Mafic lithologies exhibit greenschist facies overprints, such as retrograde growth of chlorite on garnet.

White mica weighted mean $^{40}Ar/^{39}Ar$ cooling ages of 212 ± 1 Ma, 237 ± 2 Ma, and 247 ± 2 Ma were obtained from three sample localities within this zone (Table 1; Webb et al., 1999). In addition, Eide et al. (1994) reported a phengite $^{40}Ar/^{39}Ar$ total fusion age of 231 ± 2 Ma from the D317b locality.

High- and ultrahigh-P eclogite units. The high- and ultrahigh-*P* eclogite units are characterized by penetratively deformed, compositionally distinct lithologies that outline a series of northwest-trending synforms and antiforms that are overturned to the north (Figs. 2, A and B). The antiforms are topographically expressed as elliptical domes. The domes are characterized by cores of megacrystic, quartzofeldspathic gneiss mantled by metasedimentary lithologies (including quartz-albite-muscovite schists, garnet-muscovite-biotite gneisses, marble, and minor graphitic schists) that contain blocks and boudins of eclogite. This pseudostratigraphy may represent primary layering of subducted granitic basement of the Yangtze craton and its sedimentary and volcanic cover sequences.

Both high-*P* and ultrahigh-*P* eclogite units exhibit one dominant foliation (S1) that is common both to the host gneisses and schists and to the partially retrogressed eclogite and amphibolite blocks. In felsic lithologies, S1 foliations are characterized by parallel alignment of quartz + albite + phengite (± K-feldspar ± biotite ± garnet ± epidote ± titanite). Partially retrogressed and mylonitized eclogite bodies are typified by garnet + clinopyroxene + phengite + quartz + epidote (± hornblende ± biotite ± rutile ± kyanite). S1 predominately dips moderately to shallowly southwest and northeast, reflecting folding around around lineation-subparallel, isoclinal folds (B2) that indicate high-strain deformation; the mineral stretching lineations trend southwest or southeast (Fig. 5A). In the southern region of the high-*P* eclogite unit, shear bands dip southwest and kinematic indicators such as σ clasts, δ clasts, and S-C fabrics universally show top-to-north shear (Figs. 2, 4E, and 5A). Along the northern margin of the high- and ultrahigh-*P* eclogite units, the foliation rolls over and dips north

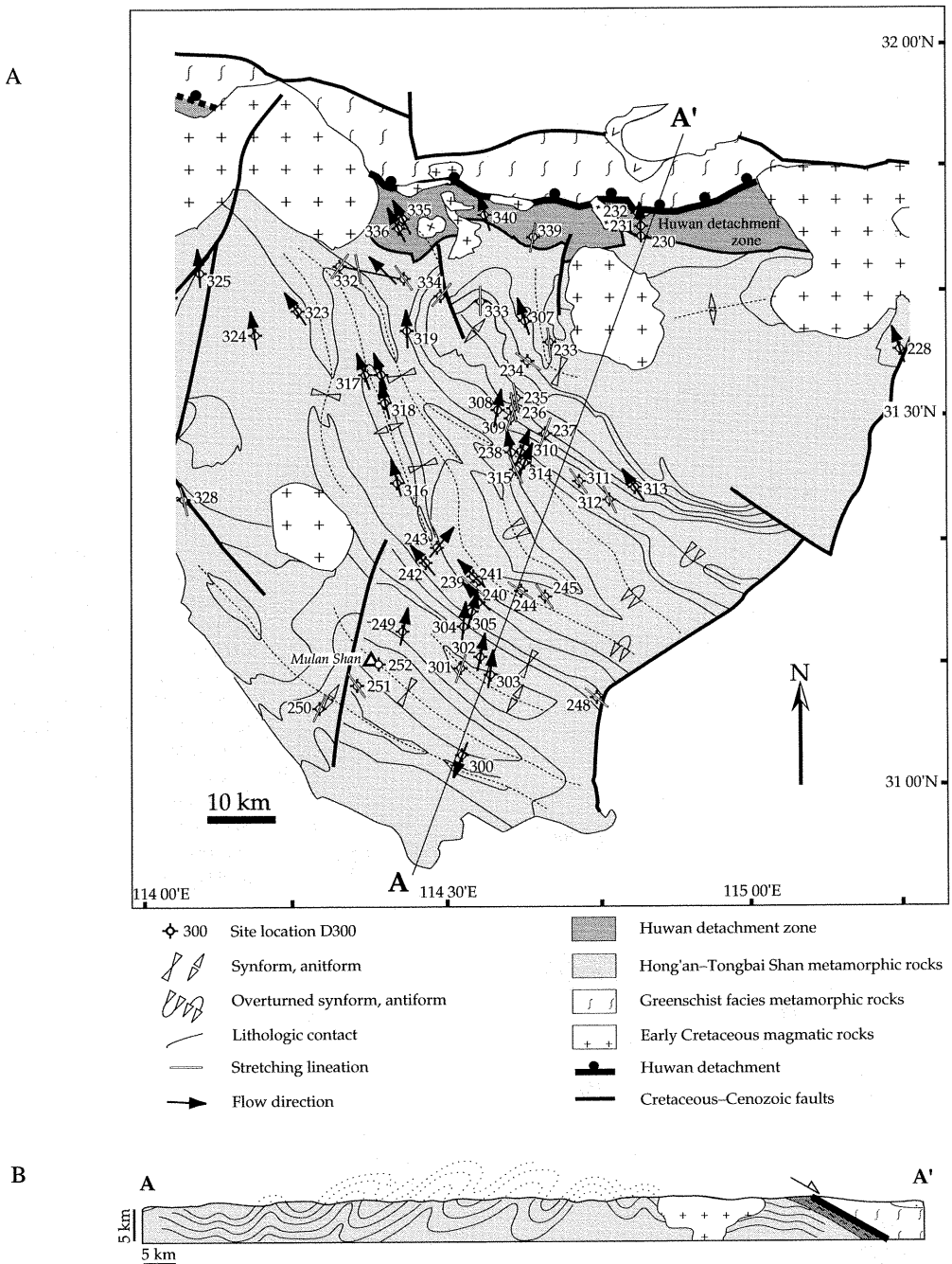

Figure 2. A: Triassic kinematic map of Hong'an region. Stereonets of structural data for individual localities are in Figures 3, 5, and 6. Black arrows portray flow direction during extensional ductile flow within high- and ultrahigh-pressure units. Lithological contacts outline large-scale folds. See Figure 1 for approximate locations of metamorphic boundaries. B: Schematic cross section across Hong'an Shan illustrating overturned folds and roll-over of foliation into north-dipping Huwan detachment. Note that section is at high angle to tectonic transport direction, which is subparallel to northwest trend of fold axes.

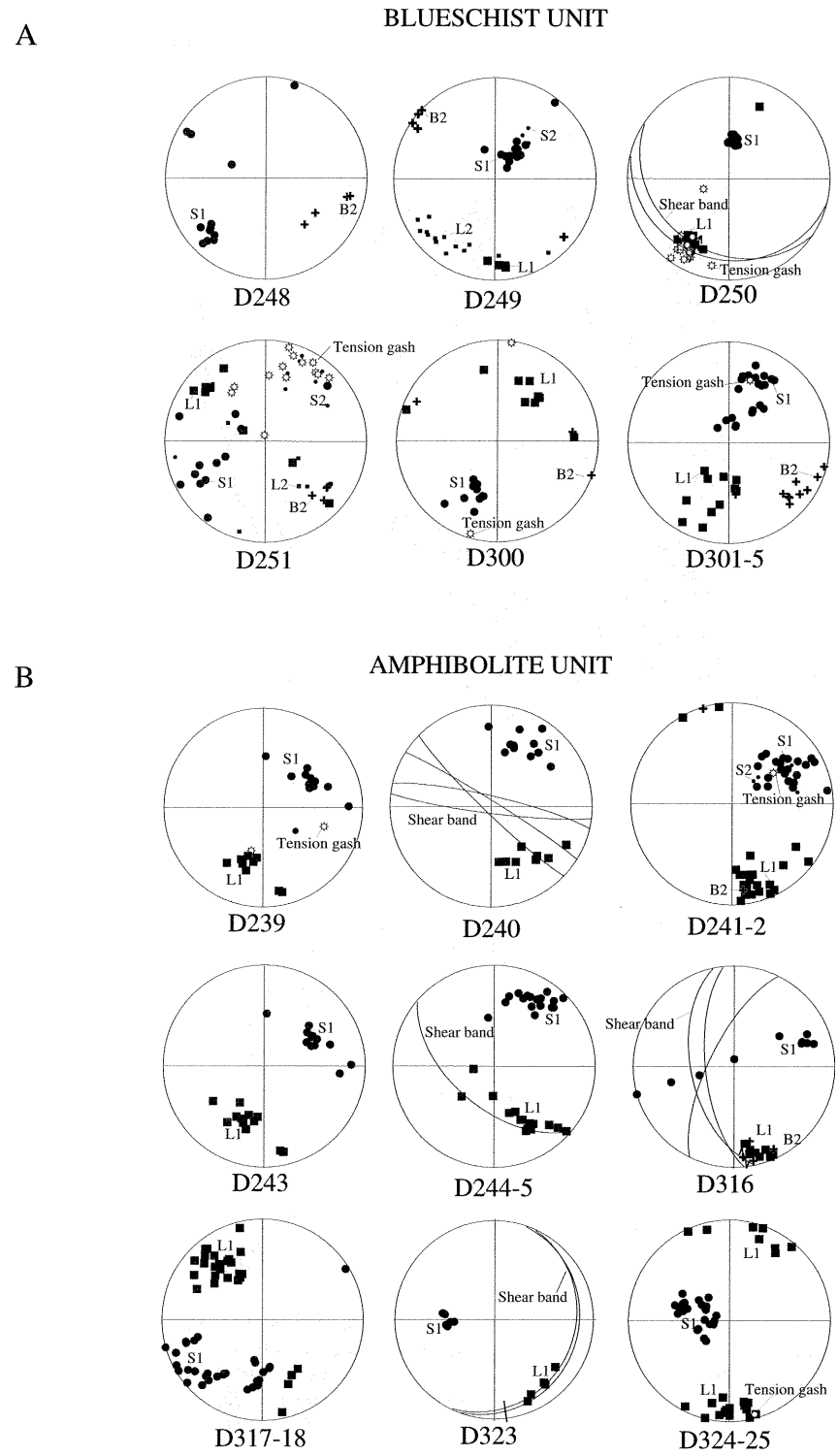

Figure 3. Structural data for (A) blueschist unit and (B) amphibolite unit represented in equal-area, lower hemisphere projections. Lettered annotations of data: S, pole to foliation (solid circles); L, stretching lineation (solid squares); B, fold axes. Number refers to generation of structure. Great circles represent shear bands. Whole, half, and headless arrows represent degree of certainty of shear-sense determination for that shear band where observed. See Figure 2 for location of structural data stations presented here.

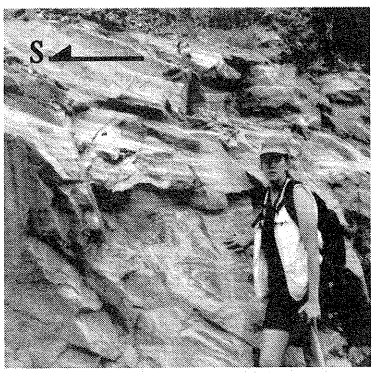

A

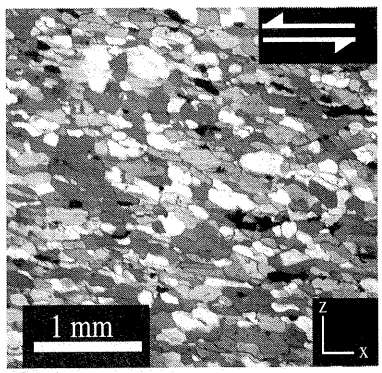

B

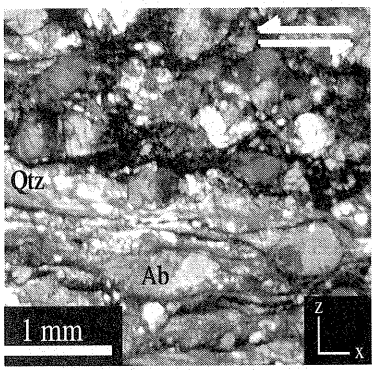

C

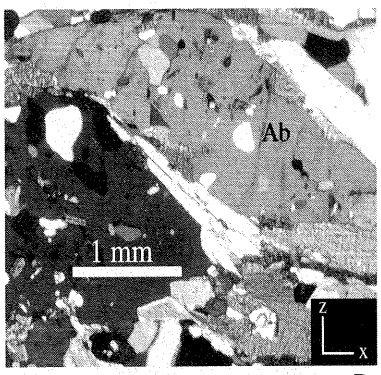

D

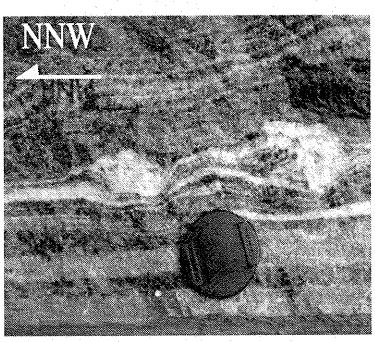

E

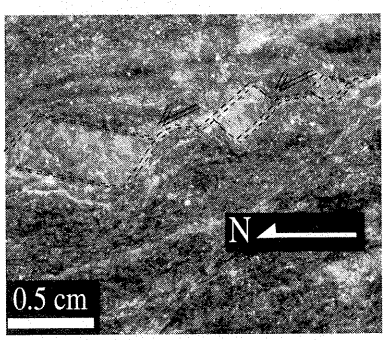

F

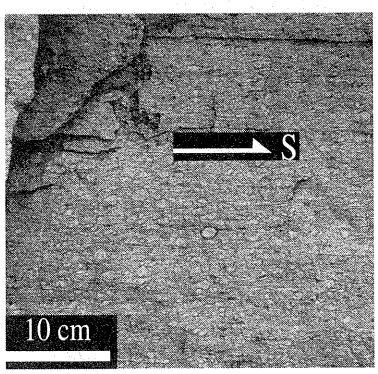

G

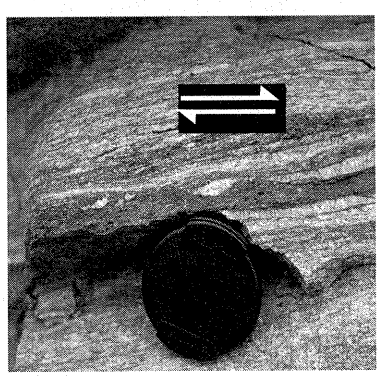

H

Figure 4. A: South-vergent, tight folds from locality D300 in blueschist unit. B: Partially annealed quartz grain-shape fabric parallel to incremental foliation (locality D301). Cut is parallel to finite lineation (X) and normal to finite foliation (Z). Inclination of quartz grains with respect to finite foliation indicates top-to-north shear sense (sinistral in reference frame of photo). C: Mantled albite porphyroclasts from mylonite in amphibolite unit indicating sinistral shear sense (sample D240b). D: Typical synkinematic to postkinematic albite porphyroblast is observed throughout amphibolite unit (sample D305b). E: Typical mesoscopic kinematic indicator in high- and ultrahigh-pressure eclogite units. Asymmetric boudinage of felsic layer in amphibolite facies gneiss gives top-to-north-northwest shear (locality D318). Diameter of lens cap is 50 mm. F: Outcrop photo of mylonitic eclogite from Huwan detachment zone (locality D335). Garnet boudins indicate top-to-north, normal-sense shear. G: Top-to-south sigma clasts formed by feldspars in gneissic core of dome (locality D253). View is parallel to lineation and normal to foliation. H: Dextral shear indicated by asymmetric boudinage of felsic layer in mylonite at locality D260. Diameter of lens cap is 50 mm.

TABLE 1. $^{40}Ar/^{39}Ar$ DATA SUMMARY

Sample number	Rock type	Mineral dated	TFA (Ma)	WMA (Ma)	IIA (Ma)	$^{40}Ar/^{36}Ar$ Intercept	MSWD
Blueschist unit							
D249C	Schist	KFS	158 ± 2	171 ± 2	170 ± 3	319 ± 82	37
Amphibolite unit							
D241A	Schist	WM	236 ± 2	237 ± 2	235 ± 2	2419 ±1344	3.1
D317B	Eclogite	WM	243 ± 2	247 ± 2	243 ± 6	528 ± 460	29
D323A	Schist	WM	213 ± 2	212 ± 1	211 ± 2	506 ± 220	20
HP-UHP eclogite units							
D228A	Gneiss	WM	205 ± 2	206 ± 2	206 ± 2	294 ± 6	0.3
D238A	Gneiss	WM	201 ± 2	203 ± 2	203 ± 2	842 ± 129	0.5
D244B	Gneiss	KFS	163 ± 2	169 ± 2	163 ± 3	338 ± 19	5.7
D307A	Eclogite	WM	218 ± 2	222 ± 2	221 ± 2	365 ± 43	1
D307B	Gneiss	WM	195 ± 2	196 ± 2	195 ± 2	543 ± 262	26
D310C	Eclogite	WM	233 ± 1	234 ± 1	234 ± 1	299 ± 13	2.6
D312A	Gneiss	WM	208 ± 1	207 ± 1	206 ± 1	383 ± 17	0.8
D332A	Shear band	WM	222 ± 2	224 ± 2	225 ± 2	143 ± 61	4.4
D332C	Shear band	WM	232 ± 2	231 ± 2	229 ± 3	405 ± 110	11
Huwan detachment zone							
D232D	Mylonite	WM	235 ± 2	234 ± 2	234 ± 2	309 ± 35	17
D335B	Shear band	WM	232 ± 2	233 ± 2	211 ± 11	4471 ± 4691	10
Dawu dome							
D253A	Gneiss	WM	195 ± 2	194 ± 2	194 ± 2	499 ± 48	2.5
D254A	Schist	WM	196 ± 2	196 ± 2	197 ± 2	258 ± 23	0.5
D326A	Gneiss	WM	198 ± 2	198 ± 2	198 ± 2	344 ± 73	12
Tongbai shear zone							
D260B	Mylonite	WM	130 ± 1	131 ± 1	132 ± 1	224 ± 19	4.6
D260C	Mylonite	KFS	120 ± 1	110 ± 1	103 ± 1	649 ± 15	2.1
D345A	Gneiss	BIO	123 ± 1	124 ± 1	124 ± 1	367 ± 61	2
D345A	Gneiss	KFS	105 ± 2	97 ± 3	96 ± 4	318 ± 71	0.5
D347A	Shear band	BIO	120 ± 1	122 ± 1	121 ± 1	423 ± 74	1
D347B	Gneiss	BIO	119 ± 1	119 ± 1	119 ± 1	289 ± 8	0.2
Late Cretaceous sinistral faults							
D256A	Mylonitized granite	KFS	83.9 ± 0.8	83.4 ± 0.8	80.5 ± 2.5	430 ± 102	6.8
D256C	Pseudotachylite	WR	75.4 ± 0.7	74.9 ± 0.8	74.9 ± 0.8	590 ± 111	0.6
Cretaceous plutons							
D321C	Granite	BIO	121 ± 1	121 ± 1	121 ± 2	300 ± 110	9.6
D321C	Granite	KFS	98 ± 1	101 ± 1	87 ± 8	846 ± 641	1.6
D342.5	Granite	BIO	118 ± 1	130 ± 1	128 ± 2	552 ± 95	1.5

Note: TFA—total fusion age; WMA—weighted mean age; IIA—inverse isochron age; $^{40}Ar/^{36}Ar$ intercept—inherited argon component, 295.5 is atmospheric $^{40}Ar/^{36}Ar$ ratio; MSWD—mean square weighted deviation, expresses goodness of fit index for inverse isochron; HP—high pressure; UHP—ultrahigh pressure; KFS—K-feldspar; WM—white mica; BIO—biotite; WR—pseudotachylite. Data are from Webb et al., 1999.

or northeast, and stretching lineations plunge subhorizontally north or northwest (Fig. 5A). Kinematic indicators imply top-to-north shear (Fig. 2A). No tectonic contact between the high- and ultrahigh-*P* eclogite units was observed in the field; thus we interpret the change in metamorphic grade to represent an isograd rather than a tectonic boundary. In thin section, felsic lithologies display dynamic recrystallization of quartz and synkinematic to postkinematic albite porphyroblasts. In samples from eclogite bodies most garnet porphyroclasts contain prograde inclusion assemblages (Zhou et al., 1993) and show retrograde amphibole coronas or chlorite overgrowths.

White mica from eclogite, schist, and gneiss yielded weighted mean $^{40}Ar/^{39}Ar$ cooling ages ranging from 231 ± 2 Ma to 196 ± 2 Ma (Table 1; Webb et al., 1999).

Huwan detachment zone. The Huwan detachment forms the northern boundary of the high- and ultrahigh-*P* rocks in the

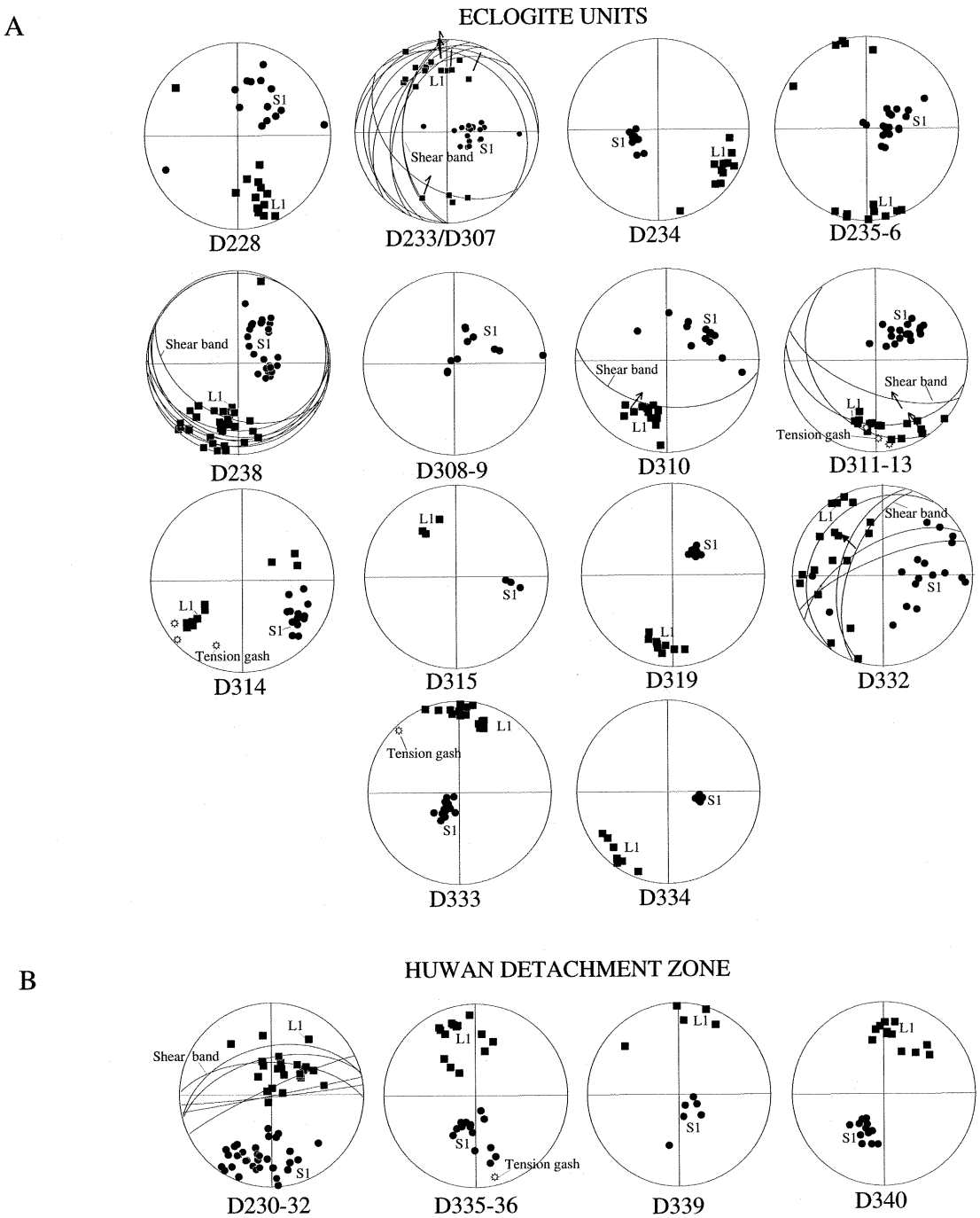

Figure 5. Structural data for (A) high- and ultrahigh-pressure eclogite units and (B) Huwan detachment zone represented in equal-area, lower hemisphere projections. Lettered annotations of data: S, pole to foliation; L, stretching lineation; B, fold axes. Number refers to generation of structure. Great circles represent shear bands. Whole, half, and headless arrows represent degree of certainty of shear-sense determination for that shear band where observed. See Figure 2 for location of structural data stations presented here.

Hong'an Shan, separating these rocks from greenschist facies metamorphic rocks to the north (Figs. 1 and 2A; Rowley and Xue, 1996; Webb et al., 1996). Rocks in the detachment zone, previously classified separately as the Sujiahe Group, were recently shown to comprise quartzofeldspathic schist and gneiss and high-*P* eclogite bodies correlating to the high- and ultrahigh-*P* units (Hacker et al., 1998). Deformation and retrogression is concentrated in an ~5-km-thick (structural thickness) deformation zone with generally north-dipping foliation and north-plunging stretching lineation (Figs. 2 and 5B). Shear bands, S-C fabrics, asymmetric boudinage, and σ and δ clasts all indicate top-to-north shear (e.g., Fig. 4F).

The detachment zone is intruded by undeformed Early Cretaceous granites. Synkinematic white mica $^{40}Ar/^{39}Ar$ cooling ages of 233 ± 2 Ma and 234 ± 2 Ma were obtained from a shear band and mylonite from the Huwan detachment zone (Table 1; Webb et al., 1999).

Dawu dome. A younger stage of deformation is observed throughout the Hong'an block and is best viewed in ductile to brittle structures at Dawu dome (Fig. 6A). The dome is characterized by a felsic gneissic core (Fig. 4G) mantled by greenschist facies metasedimentary rocks. These rocks are cut by north-dipping and south-dipping shear bands with normal-sense displacement (Fig. 6B). Ductile fabrics related to this coaxial deformation are cut by kinematically similar sets of ductile-brittle to brittle faults at and near Dawu, implying a continuum of exhumation through upper crustal depths during this tectonic episode (Fig. 6B). Late-stage quartz veins and fault arrays at localities in the blueschist and eclogite units in the Hong'an region indicate similar northeast-southwest subhorizontal extension during this stage of cooling and decompression (Fig. 6B).

Synkinematic white mica cooling ages of 196 ± 2 Ma, 195 ± 2 Ma, 198 ± 2 Ma were obtained from both the gneissic core and the metasedimentary cover of Dawu dome (Table 1; Webb et al., 1999).

Tongbai Shan. In the Tongbai Shan, a major northwest-trending shear zone involves both metasedimentary and igneous rocks, and appears to continue west toward the Qinling mountains (our observations; Regional Geological Survey [RGS] Henan, 1989). Orthogneiss at locality D347 along the southern margin of an Early Cretaceous pluton (Fig. 7A) was deformed at amphibolite facies conditions and exhibits relatively high grade, ductile fabrics. We did not observe a contact between the gneiss and the pluton in the field. A plausible explanation is that the orthogneiss is the deformed margin of a synkinematic pluton. Mylonitic, metasedimentary lithologies are found farther south and southwest, depicting lower temperature deformation farther from the pluton (Fig. 7A). Sense of shear in both the orthogneiss and metasedimentary rocks is dextral, as indicated by asymmetric boudinage, shear bands, and σ and δ clasts (Figs. 4H and 7B, localities D260, D345, and D347).

Synkinematic white mica and biotite yielded Early Cretaceous cooling ages ranging from 131 to 119 Ma (Table 1; Webb et al., 1999). K-feldspar from two localities gave weighted mean cooling ages of 110 ±1 Ma and 97 ± 3 Ma. Similar ages were obtained from Early Cretaceous plutons in the Hong'an and Tongbai Shan (Li and Wang, 1991; Eide et al., 1994; Webb et al., 1999).

A northwest-trending, sinistral strike-slip fault zone overprints the southern margin of the Tongbai dextral shear zone (Fig. 7, A and B, localities D256 and D259). The zone deforms blueschist facies rocks, Early Cretaceous plutons, and Cretaceous redbeds (RGS Hubei, 1990) under subgreenschist facies conditions. We correlate sinistral-transtensional faulting along the southern side of Dawu dome with this event (Fig. 7B). Late Cretaceous ages were obtained from a low-temperature deformed Early Cretaceous pluton and pseudotachylite cutting it (Table 1; Webb et al., 1999).

INFERRED MESOZOIC KINEMATIC EVOLUTION OF THE HONG'AN BLOCK

The collision between the Sino-Korean and Yangtze cratons is best demonstrated in the Hong'an region by the large volume of crustal rocks metamorphosed at blueschist facies to eclogite facies conditions and the preservation of coesite in ultrahigh-*P* metamorphic rocks in both the Hong'an and Dabie Shan. However, contractional structures of the appropriate age are cryptic within the interior of the orogenic belt (Xue et al., 1996). Here we interpret the overall structure of the high- and ultrahigh-*P* units to represent a warped extensional footwall, wherein top-to-northwest shear in south-dipping fabrics roll over into top-to-northwest shear in north-dipping fabrics. This implies a north-dipping continental subduction zone prior to exhumation and that all the described penetrative, Triassic–Jurassic deformation is related to exhumation along a crustal-scale normal-shear zone that encompasses the Hong'an and Dabie basement units. The extensional deformation within the interior of the orogen opposes contractional deformation in the foreland fold and thrust belt south and east of the Hong'an and Dabie Shan. The foreland structures record thrusting during the Triassic and the Jurassic, but a detailed understanding of the tectonic record is hampered by a combination of poor exposure and structural dismemberment during Cretaceous deformation (RGS Anhui, 1987; RGS Hubei, 1990; Ratschbacher et al., 2000; Schmid et al., 2000).

The oldest structures observed in the Hong'an region postdate the ultrahigh-*P* metamorphic event. The clearest link between $^{40}Ar/^{39}Ar$ ages and deformation comes from the Huwan detachment zone, where synkinematic white mica from the detachment zone yielded ages of ca. 235 Ma (Webb et al., 1999). Similarly old $^{40}Ar/^{39}Ar$ ages were reported from localities in the high- and ultrahigh-*P* rocks in both the Hong'an and Dabie Shan (Eide et al., 1994; Hacker and Wang, 1995; Webb et al., 1999). Tectonic denudation, defined as Middle to Late Triassic by $^{40}Ar/^{39}Ar$ white mica ages, was concomitant with thrusting in the foreland east and south of the Hong'an and Dabie Shan; there Middle Triassic sedimentary breccia and conglomerate,

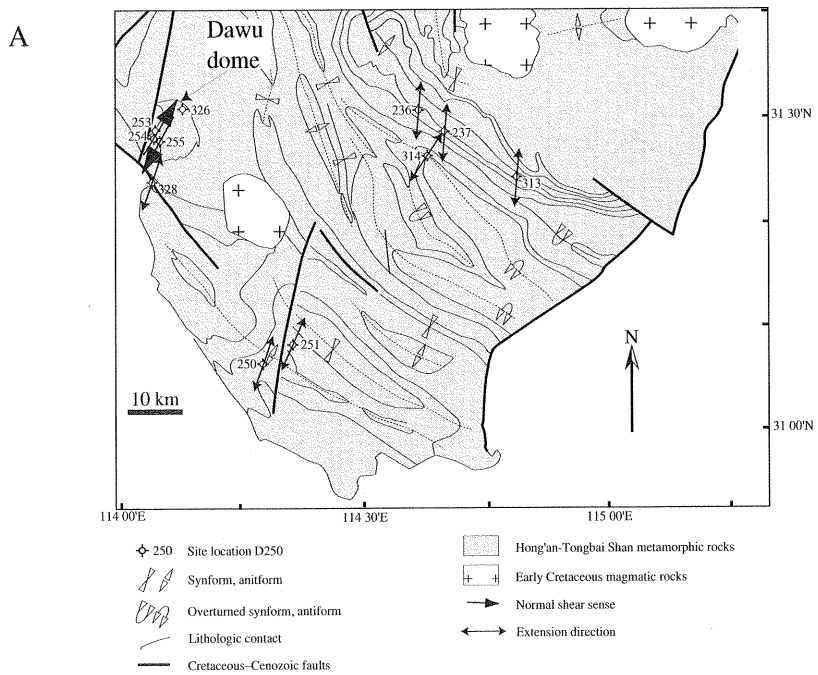

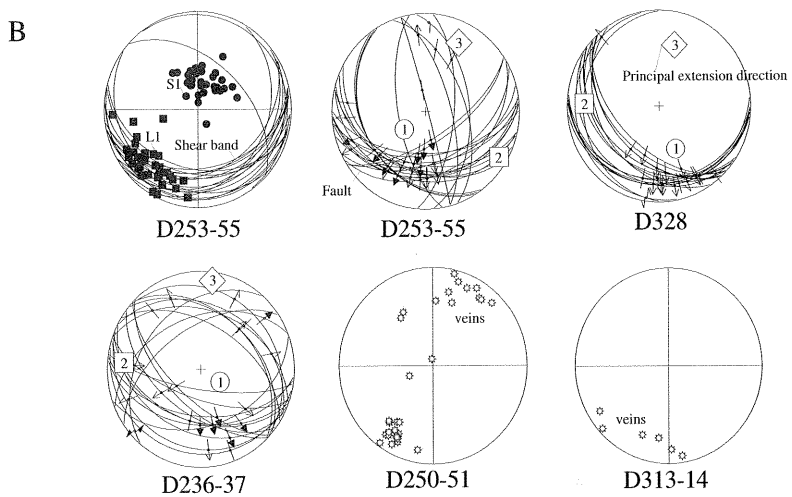

Figure 6. A: Kinematic map of Hong'an region for Early Jurassic deformation. B: Structural data plotted in equal-area, lower hemisphere projections. Lettered annotations of data: S, pole to foliation; L, stretching lineation. Number refers to generation of structure. Symbols for veins indicate poles to plane formed by tension gash. Whole, half, and headless arrows in fault data sets represent degree of certainty of slip sense determination on that fault. Principal stress directions (represented by 1, 2, and 3) were computed using fault-slip inversion techniques (see methods section in text).

deposited unconformably above Early Triassic limestone, are interpreted to date the main folding phase (Schmid et al., 2000).

Ages from synkinematic white mica in both the gneissic core and overlying metasedimentary rocks from Dawu dome indicate that the 198–194 Ma population of $^{40}Ar/^{39}Ar$ ages dates northeast-southwest extension. The subhorizontal extension direction in the ductile fabrics is identical to the extension direction during ductile-brittle to brittle faulting at Dawu (Fig. 6B) and to that determined from fault arrays and late-stage tension gashes elsewhere within the Hong'an block. The $^{40}Ar/^{39}Ar$ cooling ages and the continuum of faulting though the ductile and brittle regimes suggest that exhumation of the ultrahigh-*P* rocks through upper crustal levels occurred by the Early Jurassic in the Hong'an block. It is likely that the suite of 200–180 Ma $^{40}Ar/^{39}Ar$ ages for white mica in the Dabie Shan reported by Hacker and Wang (1995) reflects cooling during this same tectonic episode.

Early Cretaceous tectonism is most evident in the Tongbai and Dabie Shan. Extension and sinistral-oblique slip occurred from ca. 140 to 120 Ma along the Xiaotian-Mozitang fault of the northern Dabie Shan and resulted in the exhumation of rocks from depths of ~15 km (Ratschbacher et al., 2000). We suggest that this fault is the eastward continuation of the Huwan detachment that was reactivated and overprinted during Cretaceous extension and plutonism. Consequently, high- and ultrahigh-*P* rocks that resided at deeper crustal levels for a longer period of time are now exposed in the Dabie Shan, as

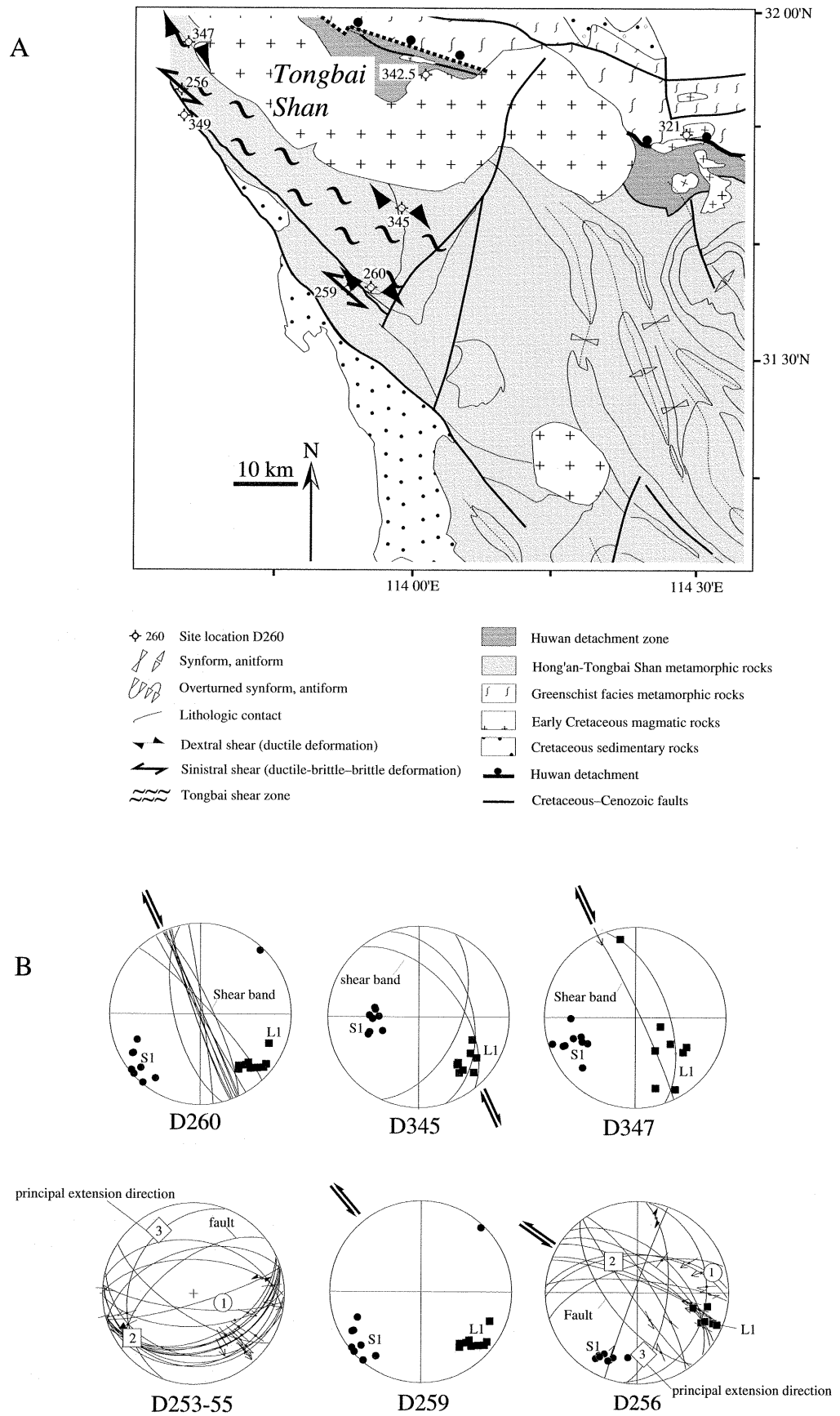

Figure 7. A: Cretaceous kinematic map of Tongbai and Hong'an Shan. B: Structural data are represented in equal-area, lower hemisphere projections. See Figures 3 and 6 for explanation of symbols and lettering used.

opposed to the Hong'an and Tongbai Shan, where Cretaceous deformation involved primarily strike-slip motion and little or no tectonic exhumation.

Dextral shear along the southwestern margin of the Tongbai Shan coeval with sinistral shear along Xiaotian-Mozitang fault of the northern margin of the Dabie Shan would have resulted in eastward lateral extrusion of the interior units of the Tongbai, Hong'an, and Dabie Shan. This tectonism may have been driven by the Jurassic–Cretaceous collision of the Lhasa block with Eurasia (Allegrè et al., 1984).

Late Cretaceous $^{40}Ar/^{39}Ar$ ages obtained for the low-temperature sinistral strike-slip faults along the southern margin of the Tongbai Shan are corroborated by Cretaceous–Eocene apatite fission-track data reported by Ames (1995). In addition, Hacker et al. (1995) reported that sinistral strike-slip faults form the boundary between blueschist facies rocks and the foreland fold and thrust belt in the southern Dabie Shan. Although not significant in the exhumation history of the ultrahigh-*P* rocks, this Late Cretaceous tectonism formed major block-bounding faults for the Dabie Shan, Hong'an, and Tongbai regions.

Implications for exhumation models

The structural data presented here suggest that high- and ultrahigh-*P* rocks of the Hong'an and Dabie Shan were exhumed as a single, penetratively deformed slab bounded at the top by a north-dipping detachment fault zone. Models incorporating this scenario were previously published for the Dabie Shan (e.g., Maruyama et al., 1994; Ernst and Peacock, 1996; Liou et al., 1996), but lacked substantiating structural evidence. In these models, reminiscent of the physical models by Chemenda et al. (1995, 1996), exhumation is driven by buoyancy forces due to density contrasts between the subducted crustal rocks and the overlying mantle lithosphere, and/or continued contraction during collision. This general model is attractive for explaining the preservation of ultrahigh-*P* rocks in that cooling of the exhumed slab is achieved across both upper and lower surfaces (Fig. 8;

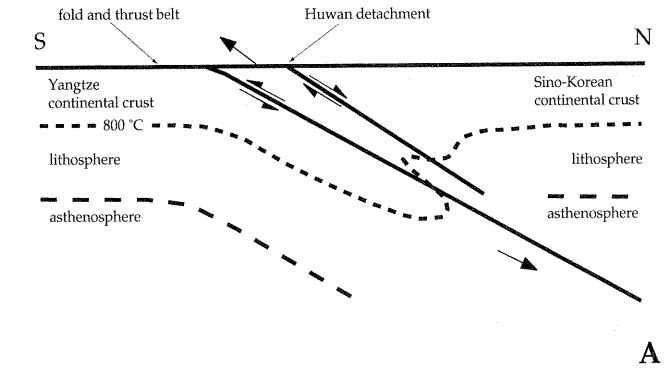

A

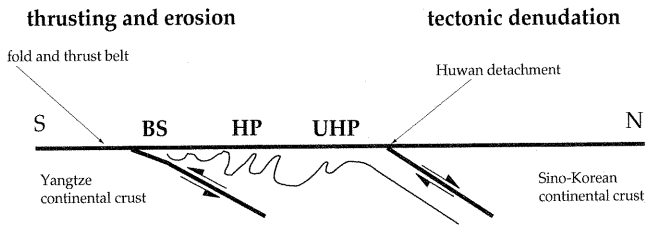

B

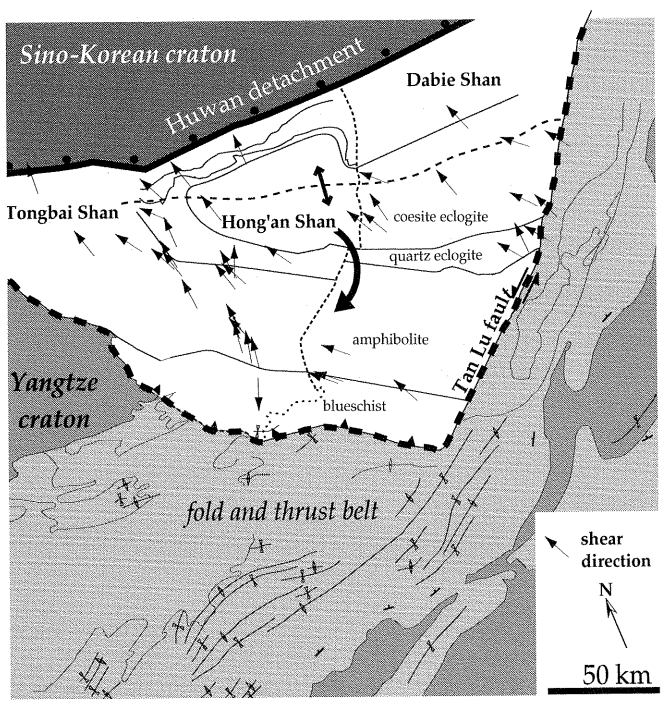

C

Figure 8. Schematic tectonic model for exhumation of blueschist (BS) unit, and high-pressure (HP) and ultrahigh-pressure (UHP) eclogite units. A: Figure is modified from Ernst and Peacock (1996). Bowed isotherm illustrates how cooling is achieved along upper and lower boundaries of exhuming slab as HP and UHP rocks come into contact with cooler rocks. B: Structures and relative locations of metamorphic units in Hong'an Shan resulting from exhumation. Unroofing is accompanied by thrusting and erosion within fold and thrust belt south and east of Hong'an and Dabie Shan and by normal shear within HP and UHP units and along Huwan detachment zone. Note that section is at an angle to tectonic transport direction, thus a component of exhumation occurs subnormal to section plane. C: Pre-Cretaceous restoration of Tongbai, Hong'an, and Dabie Shan modified after Hacker et al. (1998). Arrow represents clockwise rotation of slab during exhumation. In this model, Tan Lu fault originates in Middle to Late Triassic as sinistral transfer fault that accommodates extension and continued contraction in foreland as collision progresses westward.

Ernst and Peacock, 1996). Coeval extension along the Huwan detachment and shortening in the foreland require accommodation structures of the same age. One possibility is the initiation of the Tan Lu fault in the Middle to Late Triassic as a sinistral transfer fault (Fig. 8C). The paleomagnetic data suggesting clockwise rotation of the Tongbai, Hong'an, and Dabie Shan (Enkin et al., 1992) are compatible with this model.

The comprehensive structural studies and radiometric age data, summarized here and detailed in Hacker et al. (1998, 2000) and Webb et al. (1999), suggest that exhumation from mantle depths of 120–150 km to crustal depths occurred between ca. 245–240 Ma and ca. 235–230 Ma.

CONCLUSIONS

Evidence of multiple Mesozoic tectonic events affecting rocks in the Hong'an and Tongbai Shan is preserved in structural, petrologic, and radiometric age data. Early Triassic high- and ultrahigh-*P* metamorphism occurred during subduction of crustal rocks to mantle depths during collision. Middle to Late Triassic structures in the high- and ultrahigh-*P* units are associated with extension within the basement units of the Tongbai, Hong'an, and Dabie Shan and along the Huwan detachment zone that was synchronous with contraction in the foreland. Northwest-down, normal-sense shear along the Huwan detachment at the northern edge of the Hong'an block occurred ca. 235 Ma, on the basis of white mica cooling ages. The bulk of the mountain range is a warped extensional footwall, within which muscovites cooled by 205 Ma following Late Triassic–Early Jurassic retrograde metamorphism at mid-crustal levels. Younger, northeast-southwest subhorizontal extension is recorded by both ductile and brittle structures, best seen at Dawu. The associated white mica recrystallization at ca. 195 Ma and the continuum to low-temperature deformation suggest that exhumation of the high- and ultrahigh-*P* rocks through upper crustal levels occurred during Early Jurassic time. Early Cretaceous dextral shearing in the Tongbai Shan was synchronous with normal to sinistral-oblique shear along the Xiaotian-Mozitang fault of the northern Dabie Shan and syntectonic plutonism throughout the orogen. Late Cretaceous–Eocene deformation included strike-slip faulting and extension. Structures related to this deformation formed the major block-bounding faults for the Dabie Shan, Hong'an, and Tongbai regions.

ACKNOWLEDGMENTS

This work was supported by the U.S. National Science Foundation grant EAR-9417958, German National Science Foundation grants Ra442/4-1, Ra442/6-1/2, Ra442/9-1, Stanford-China Geosciences Industrial Affiliates, and a grant from the Stanford University McGee Fund. Special thanks to Mary Leech and Peng Lianhong for their assistance during the 1996 field season and to Marc Hendrix, Elizabeth Eide, and Steve Sheriff for thorough and constructive reviews of the manuscript.

REFERENCES CITED

Allegrè, C.J., and 35 others, 1984, Structure and evolution of the Himalaya-Tibet orogenic belt: Nature, v. 307, p. 17–22.

Ames, L., 1995, Geochronology and isotopic character of ultrahigh-pressure metamorphism with implications for collision of the Sino-Korean and Yangtze cratons, central China [Ph.D. thesis]: Santa Barbara, University of California at Santa Barbara, 124 p.

Ames, L., Zhou, G., and Xiong, B., 1996, Geochronology and isotopic character of ultrahigh-pressure metamorphism with implications for collision of the Sino-Korean and Yangtze cratons, central China: Tectonics, v. 15, p. 472–489.

Angelier, J., 1994, Fault-slip analysis and paleostress reconstruction, *in* Hancock, P.L., ed., Continental deformation: Tarrytown, New York, Pergamon, p. 53–100.

Chemenda, A.I., Mattauer, M., Malavieille, J., and Bokun, A.N., 1995, A mechanism for syn-collisional rock exhumation and associated normal faulting: Results from physical modeling: Earth and Planetary Science Letters, v. 132, p. 225–232.

Chemenda, A.I., Mattauer, M., and Bokun, A.N., 1996, Continental subduction and a mechanism for exhumation of high-pressure metamorphic rocks: New modeling and field data from Oman: Earth and Planetary Science Letters, v. 143, p. 173–182.

Chen, W., Harrison, T.M., Heizler, M.T., Liu, R., Ma, B., and Li, J., 1992, The cooling history of mélange zone in north Jiansu–south region: Evidence from multiple diffusion domain $^{40}Ar/^{39}Ar$ thermal geochronology: Acta Petrologica Sinica, v. 8, p. 1–17.

Dong, S., 1989, The general features and distributions of the glaucophane schist belts of China: Acta Geologica Sinica, v. 3, p. 273–284.

Eide, E.A., 1993, Petrology, geochronology, and structure of high-pressure metamorphic rocks in Hubei Province, east-central China, and their relationship to continental collision [Ph.D. thesis]: Stanford, California, Stanford University, 235 p.

Eide, E.A., McWilliams, M.O., and Liou, J.G., 1994, $^{40}Ar/^{39}Ar$ geochronologic constraints on the exhumation of high-pressure–ultrahigh-pressure metamorphic rocks in east-central China: Geology, v. 22, p. 601–604.

Enkin, R.J., Yang, Z., Chen, Y., and Courtillot, V., 1992, Paleomagnetic constraints on the geodynamic history of the major blocks of China from the Permian to the present: Journal of Geophysical Research, v. 97, p. 13953–13989.

Ernst, W.G., and Peacock, S.M., 1996, A thermotectonic model for preservation of ultrahigh-pressure phases in metamorphosed continental crust, *in* Bebout, G.E., Scholl, D.W., Kirby, S.H., and Platt, J.P., eds., Subduction top to bottom: American Geophysical Union Geophysical Monograph 96, p. 171–178.

Ernst, W.G., Zhou, G., Liou, J.G., Eide, E., and Wang, X., 1991, High-pressure and superhigh-pressure metamorphic terranes in the Qinling-Dabie mountain belt, central China; early to mid-Phanerozoic accretion of the western Paleo-Pacific Rim: Pacific Science Association Information Bulletin, v. 43, p. 6–15.

Hacker, B.R., and Peacock, S.M., 1994, Creation, preservation, and exhumation of coesite-bearing, ultrahigh-pressure metamorphic rocks, *in* Coleman, R.G., and Wang, X., eds., Ultrahigh pressure metamorphism: Cambridge, Cambridge University Press, p. 159–181.

Hacker, B.R., and Wang, Q., 1995, Ar/Ar geochronology of ultrahigh-pressure metamorphic rocks in central China: Tectonics, v. 14, p. 994–1006.

Hacker, B.R., Ratschbacher, L., Webb, L.E., and Dong, S., 1995, What brought them up? Exhumation of the Dabie Shan ultrahigh-pressure rocks: Geology, v. 23, p. 43–46.

Hacker, B.R., Wang, X., Eide, E.A., and Ratschbacher, L., 1996, Qinling-Dabie ultrahigh-pressure collisional orogen, *in* Yin, A., and Harrison, T.M., eds., Tectonic evolution of Asia: Englewood Cliffs, New Jersey, Prentice-Hall, p. 345–370.

Hacker, B.R., Ratschbacher, L., Webb, L.E., Ireland, T., Walker, D., and Dong, S., 1998, U/Pb zircon ages constrain the architecture of the ultrahigh-pressure Qinling-Dabie orogen, China: Earth and Planetary Science Letters, v. 161, p. 215–230.

Hacker, B.R., Ratschbacher, L., Webb, L.E., McWilliams, M., Ireland, T., Calvert, A., Dong, S., Wenk, H.-R., and Chateigner, D., 2000, Exhumation of the ultrahigh-pressure continental crust in east-central China: Late Triassic–Early Jurassic extension: Journal of Geophysical Research, v. 105, p. 13339–13364.

Li, S., and Wang, T., 1991, Geochemistry of granitoids in the Tongbaishan-Dabieshan, central China: Wuhan, China University of Geosciences Press, 208 p.

Li, S., Hart, S.R., Liu, D., Zhang, G.W., and Guo, A., 1989, Timing of collision between the north and south China blocks—The Sm-Nd isotropic age evidence: Scientia Sinica, ser. B, v. 32, p. 1393–1400.

Li, S., Xiao,Y., Liou, D., Chen, Y., Ge, N., Zhang, Z., Sun, S., Cong, B., Zhang, R., Hart, S.R., and Wang, S., 1993, Collision of the North China and Yangtze and formation of coesite-bearing eclogites: Timing and processes: Chemical Geology, v. 109, p. 89–111.

Lin, J.L., Fuller, M., and Zhang, W., 1985, Preliminary Phanerozoic polar wander paths for the North and South China blocks: Nature, v. 313, p. 444–449.

Liou, J.G., Zhang, R.Y., Wang, X., Eide, E.A., Ernst, W.G., and Maruyama, S., 1996, Metamorphism and tectonics of high-pressure and ultra-high-pressure belt in the Dabie-Sulu region, China, *in* Yin, A., and Harrison, T.M., eds., Tectonic evolution of Asia: Englewood Cliffs, New Jersey, Prentice-Hall, p. 300–344.

Maruyama, S., Liou, J.G., and Zhang, R., 1994, Tectonic evolution of the ultrahigh-pressure (ultrahigh-*P*) and high-pressure (high-*P*) metamorphic belts from central China: Island Arc, v. 4, p. 112–121.

Mattauer, M.P., Matte, H., Maluski, Z., Xu, X., Lu., Y., and Tang, Y., 1985, Tectonics of the Qinling Belts, build-up and evolution of eastern Asia: Nature, v. 327, p. 496–500.

Okay, A.I., Şengör, A.M.C., and Satir, M., 1993, Tectonics of an ultrahigh-pressure metamorphic terrane: Dabie Shan, China: Tectonics, v. 12, p. 1320–1334.

Opdyke, N.D., Huang, K., Xu, G., Zhang, W.Y., and Kent, D.V., 1986, Paleomagnetic results from the Triassic of the Yangtze Platform: Journal of Geophysical Research, v. 91, p. 9553–9568.

Passchier, C.W., 1982, Mylonitic deformation in the Saint-Barithélemy Massif, French Pyrenees, with emphasis on the genetic relationship between ultramylonite and pseudotachylite: Amsterdam, GUA Papers of Geology, ser. 1, v. 16, p. 1–173.

Passchier, C.W., and Trouw, R.A.J., 1996, Microtectonics: New York, Springer, 289 p.

Platt, J.P., 1986, Dynamics of orogenic wedges and the uplift of high-pressure metamorphic rocks: Geological Society of America Bulletin, v. 97, p. 1037–1053.

Ratschbacher, L., Hacker, B.R., Webb, L.E., McWilliams, M., Ireland, T., Dong, S., Calvert, A., Chateigner, D., and Wenk, H.-R., 2000, Exhumation of the ultrahigh-pressure continental crust in east-central China: Cretaceous and Cenozoic unroofing and the Tan-Lu fault: Journal of Geophysical Research, v. 105, p. 13303–13338.

Regional Geological Survey Anhui, 1987, Regional geology of the Henan Province: Beijing, Geological Publishing House, 721 p.

Regional Geological Survey Henan, 1989, Regional geology of the Henan Province: Beijing, Geological Publishing House, 726 p.

Regional Geological Survey Hubei, 1990, Regional geology of the Hubei Province: Beijing, Geological Publishing House, 705 p.

Rowley, D.B., and Xue, F., 1996, Modeling the exhumation of ultra-high pressure metamorphic assemblages; observations from the Dabie/Tongbai region, China: Geological Society of America Abstracts with Programs, v. 28, no. 7, p. 249.

Rowley, D.B., Xue, F., Tucker, R.D., Peng, Z.X., Baker, J., and Davis, A., 1997, Ages of ultrahigh pressure metamorphism and protolith orthogneisses from eastern Dabie Shan: U/Pb zircon geochronology: Earth and Planetary Science Letters, v. 151, p. 191–203.

Schmid, J.C., Ratschbacher, L., Hacker, B.R., Gaitzsch, I., and Dong, S., 2000, How did the foreland react? Exhumation of the Dabie Shan ultrahigh-pressure continental crust and the Yangtze foreland fold-and-thrust belt (eastern China): Terra Nova, v. 11, p. 266–272.

Tullis, J.R., and Yund, A., 1991, Diffusion creep in feldspar aggregates: Experimental evidence: Journal of Structural Geology, v. 13, p. 987–1000.

Wang, X., and Liou, J.G., 1991, Regional ultrahigh-pressure coesite-bearing eclogitic terrane in central China: Evidence from country rocks, gneiss, marble and metapelite: Geology, v. 19, p. 933–936.

Webb, L.E., Hacker, B.R., Ratschbacher, L., and Dong, S., 1996, Structures and kinematics of exhumation; ultrahigh-pressure rocks in the Hong'an Block of Qinling-Dabie orogen, China: Geological Society of America Abstracts with Programs, v. 28, no. 7, p. 69.

Webb, L.E., Hacker, B.R., Ratschbacher, L., McWilliams, M.O., and Dong, S., 1999, Thermochronologic constraints on deformation and cooling history of high- and ultrahigh-pressure rocks in the Qinling-Dabie orogen, eastern China: Tectonics, v. 18, p. 621–638.

Xu, S., and Su, W., 1997, Raman determination on micro-diamond in eclogite from the Dabie Mountains, eastern China: Chinese Science Bulletin, v. 42, p. 87.

Xu, S., Okay, A.I., Ji, S., Şengör, A.M.C., Su, W., Liu, Y., and Jiang, L., 1992, Diamond from the Dabie Shan metamorphic rocks and its implication for tectonic setting: Science, v. 256, p. 80–82.

Xue, F., Rowley, D.B., and Baker, J., 1996, Refolded syn-ultrahigh-pressure thrust sheets in the south Dabie complex, China: Field evidence and tectonic implications: Geology, v. 24, p. 455–458.

Xue, F., Rowley, D.B., Tucker, R.D., and Peng, Z.X., 1997, U-Pb zircon ages of granitoid rocks in the North Dabie Complex, eastern Dabie Shan, China: Journal of Geology, v. 105, p. 744–753.

Yin, A., and Nie, S., 1993, An indentation model for the North and South China collision and the development of the Tanlu and Honam fault systems, eastern Asia: Tectonics, v. 12, p. 801–813.

Zhai, X., Day, H., Hacker, B.R., and You, Z., 1998, Paleozoic metamorphism in the Qinling orogen, Tongbai Mountains, central China: Geology, v. 26, p. 371–374.

Zhang, Y.Q., Vergely, P., Mercier, J., and Ben-Avraham, Z., 1995, Active faulting in and along the Qinling Range (China) inferred from SPOT imagery analysis and extrusion tectonics of South China: Tectonophysics, v. 243, p. 69–95.

Zhou, G., Liu, J., Eide, E.A., Liou, J.G., and Ernst, W.G., 1993, High-pressure/low-temperature metamorphism in northern Hube Province, central China: Journal of Metamorphic Petrology, v. 11, p. 561–574.

MANUSCRIPT ACCEPTED BY THE SOCIETY JUNE 5, 2000

Printed in the U.S.A.